Bulletin of the Geological Society of Finland, Vol. 91, 2019, pp 179–198, https://doi.org/10.17741/bgsf/91.2.002

The 1.79 Ga Särkilahti leucogranite – a horizontal magma layer below granulite-grade migmatites in SE Finland

Hannu Mäkitie[1*], Hugh O'Brien[1], Olavi Selonen[2] and Matti Kurhila[1]

[1]*Geological Survey of Finland (GTK), P.O. Box 96, FI-02151 Espoo, Finland*
[2]*Åbo Akademi University, Department of Natural Sciences, Geology and Mineralogy, FI-20500 Turku, Finland.*

VERTAISARVIOITU
KOLLEGIALT GRANSKAD
PEER-REVIEWED
www.tsv.fi/tunnus

Abstract

The heterogeneous, peraluminous Särkilahti garnet-cordierite leucogranite occupies ~ 75 km^2 area in Svecofennian granulite-grade terrain of SE Finland. Country rocks are metasedimentary garnet-cordierite-biotite migmatites with some orthopyroxene-garnet paragneisses and orthopyroxene metatonalites. The leucogranite represents the exhumed upper portion of an extensive horizontal magma layer in the crust. Regional-scale heat flow (initiated by energy input from the mantle) caused the formation of this magma layer and it also gave rise to granulite-grade migmatization (formation of in-situ leucosomes) in the above country rocks by heat conduction. When the magma layer slowly rose, country rocks at its upper limit were melted and partly merged in the magma. Within the magma layer, lighter granitic melt ascended as a consequence of the residue sinking. Late-stage crystallization products of the layer resulted in cross-cutting granite dykes in the above migmatites. U–Pb ages on monazite for the Särkilahti leucogranite samples are 1.79–1.78 Ga. The age slightly postdates the culmination of the regional metamorphism (1.84–1.80 Ga). As the leucogranite (magma layer) represents the lowest horizontal rock unit, it has – during crustal exhumation – crystallized slightly after the peak of the regional metamorphism.

Key words: leucogranite, migmatite, partial melting, metamorphism, magma emplacement, molten crust, U–Pb geochronology, Finland

*Corresponding author (e-mail: hannu.makitie@gtk.fi)

Editorial handling: Alexander Slabunov (slabunov@krc.karelia.ru)

1. Introduction

Peraluminous granite intrusions in high-grade gneiss terrains are often explained as rooted in the migmatites or else they represent ascended accumulations of magmas that initially formed by partial melting of fertile crust (e.g. Brown, 2013, and references there in). In an alternative view, Chen and Grapes (2007) introduced the felsic "magma layer" concept, which refers to an extensive horizontal in-situ melting in the crust without notable ascent of melts into large magma chambers higher up. Thus there seems to be a divergence on how to interpret outcropping granite areas; ascended intrusion or in-situ melted magma layer? In addition, the details of the processes of extraction, transport and emplacement of granitic melt in the crust are still debated, for example in terms of feed channels and space problem (see e.g. Hobbs & Ord, 2010; Brown, 2013; Morfin et al., 2013). Anyway, field observations of the contact areas of granites are still crucial in understanding on (1) how these felsic magmas – so voluminous in continental crust – have been emplaced and (2) how the associated crustal energy input, i.e. heat flow, has affected the country rocks.

The present article describes the contact and edge areas, chemical composition, U–Pb age data and emplacement – based on an extensive horizontal magma layer below granulite-grade migmatites – of the Paleoproterozoic Särkilahti garnet-cordierite leucogranite (~ 75 km^2 in extent) (Mäkitie et al., 2016) located in a Svecofennian terrain (Nykänen, 1988; Hölttä & Heilimo, 2017) in SE Finland. The study area belongs to a 100 km wide and 500 km long late Svecofennian granite-migmatite zone of southern Finland, which is characterized by 1.84–1.79 Ga microcline granites (including the Särkilahti leucogranite) in high-grade gneiss terrains derived from 1.91–1.87 Ga old metasedimentary and -volcanic rocks (e.g. Ehlers et al., 1993; Kurhila et al., 2005, 2011, and references there in) (Fig. 1). Finally, we discuss the interactions between the leucogranite emplacement and the practically coeval granulite-grade metamorphism in the country rocks with a crustal cross-section.

2. Regional geological setting

The Särkilahti region is located in the eastern part of the extensive granite-migmatite zone of southern Finland described by Ehlers et al. (1993). The granites of the zone often form irregular areas; for this reason the margins of them cannot usually be precisely defined. The granites are recently interpreted as "continental granites" (Nironen et al., 2016), and earlier as "intrusions postdating the main stage of crustal thickening" (Korsman et al., 1997). Nurmi and Haapala (1986) concluded that these granites were formed when Proterozoic sedimentary rocks were partially melted in the continental crust. The high-grade metamorphism and magmatism of southern Finland are thought to be a result of crustal extension, leading to a high heat flow from the mantle (Korsman et al., 1999; Lahtinen et al., 2005), or of a combined effect of crystal thickening and radioactive heat production (Kukkonen & Lauri, 2009). In general, the granites of the granite-migmatite zone crystallized 1.84–1.80 Ga ago, and during this period their country rocks underwent metamorphism, which P-T conditions vary from middle amphibolite to granulite facies (e.g. Nironen, 2017; Hölttä & Heilimo, 2017, and references there in).

More detailed studies of the emplacement and age of the afore-mentioned granites have so far mainly concentrated on the western part of the granite-migmatite zone of southern Finland (see Ehlers et al., 1993; Selonen et al., 1996; Väisänen et al., 2002; Johannes et al., 2003; Stålfors & Ehlers, 2006; Nironen & Kurhila, 2008). This study of the Särkilahti leucogranite is located in the eastern part of the zone (Fig. 1), where the related granites usually occupy irregular areas (see e.g. Nykänen, 1987; Lavikainen et al., 1992). The Särkilahti region is part of a wide granulite-grade zone, where rocks have undergone regional metamorphism in 4–6 kbar and ~ 800 °C, resulting in migmatites 1.84–1.80 Ga ago (Hölttä & Heilimo, 2017; Nironen, 2017). Additionally, the region had undergone earlier metamorphism, associated with the intrusion of tonalite bodies 1.90–1.88 Ga

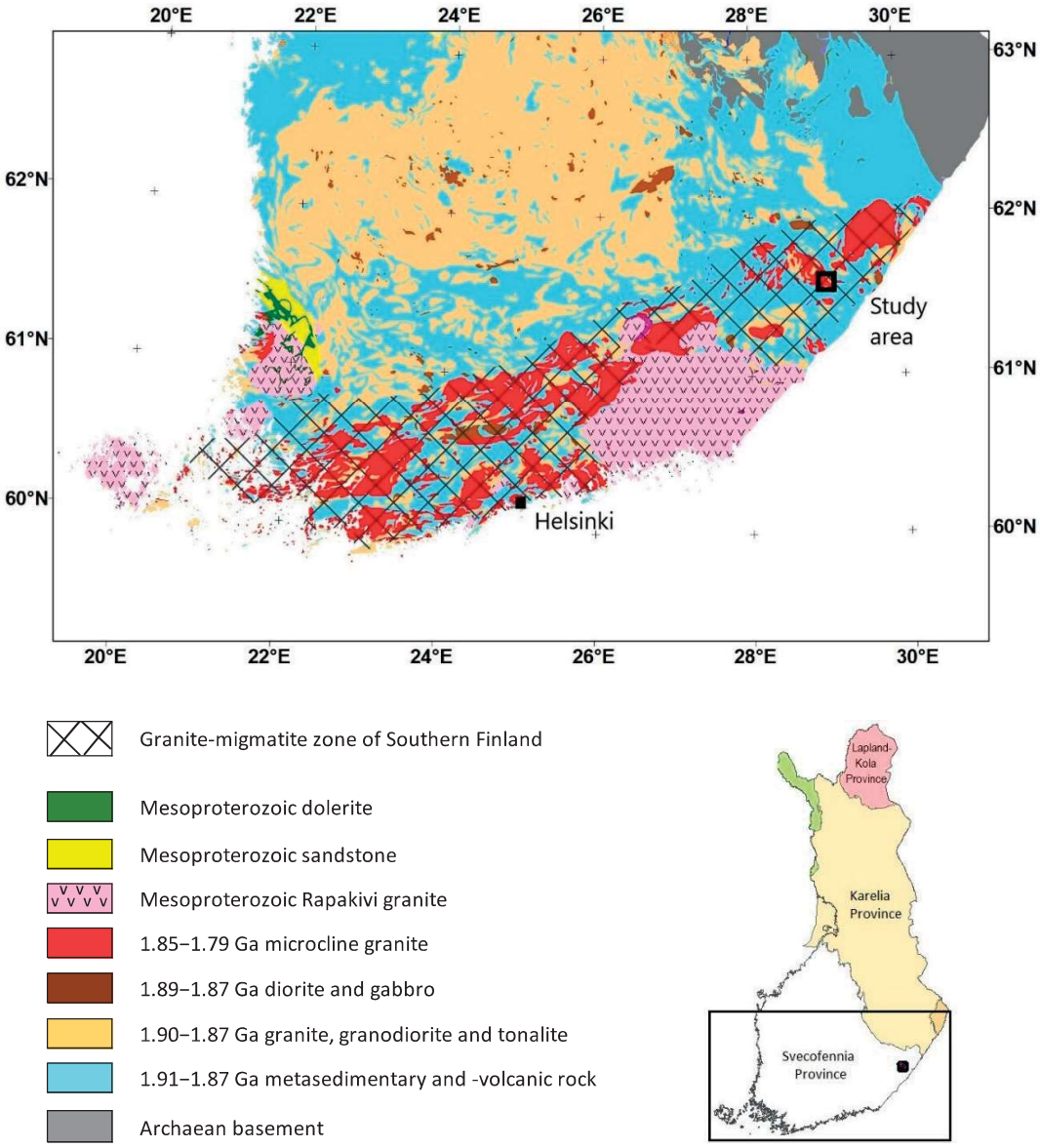

Figure 1. Simplified geological map of southern Finland (after DigiKP200 database of the Geological Survey of Finland). The extent of the 100 km wide and 500 km long granite-migmatite zone of Southern Finland (Ehlers et al., 1993) is illustrated by a grid. The study area is also marked as a black square in the small map of main tectonic provinces of Finland after Luukas et al. (2017).

ago (Korsman et al., 1984). Geographically, the Särkilahti region is located 30 km south of the town of Savonlinna in SE Finland.

Metatexitic garnet-cordierite-biotite migmatite is the typical country rock of the Särkilahti leucogranite, with a lesser amount of orthopyroxene-garnet paragneisses and pyroxene metatonalites (Fig. 2) (Nykänen, 1987, 1988; Selonen, 1988; Lavikainen et al., 1992). The protoliths to the migmatites and paragneisses were initially deposited 1.91–1.87 Ga ago, and were intruded by tonalites at 1.90–1.87 Ga (Nironen et al., 2016;

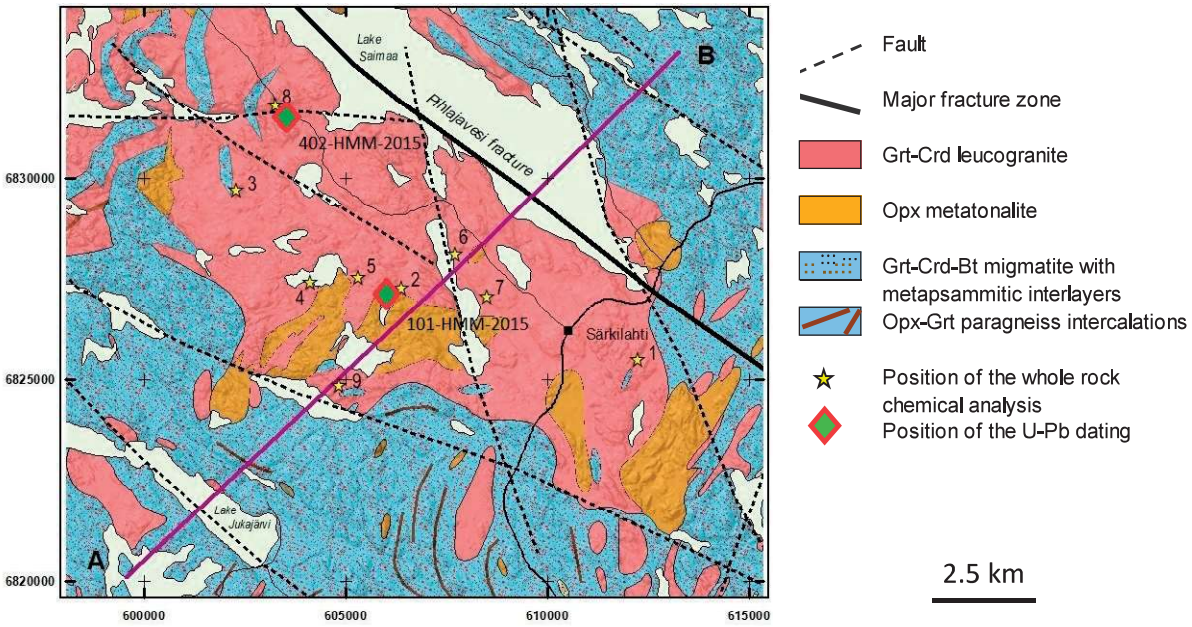

Figure 2. Geological map of the study area (modified after Nykänen, 1988; Lavikainen et al., 1992). The Särkilahti leucogranite occupies the central part of the map. Lilac-colored line A-B refers to position of the crustal cross-section shown in Figure 13. Sites of the chemically analyzed granites are marked as yellow stars, with codes referring to column numbers in Table 1.

Nironen, 2017). Aeromagnetic data indicate that the leucogranite and metatonalite exhibit slightly stronger magnetic signatures compared to those characterized by the migmatites.

According to the major stratigraphic units of the bedrock of Finland (Luukas et al., 2017 and Finstrati database), the Särkilahti leucogranite is part of a large lithodeme called "undefined granite". This lithodeme refers to the numerous "microcline granite" areas in the granite-migmatites zone shown in Fig. 1. The microcline granites belong to the slightly larger Southern Finland granite suite. The garnet-cordierite-biotite migmatites, on the other hand, are classified as belonging to the "undefined biotite paragneiss" lithodeme of the large Häme migmatite suite.

Several elongated valleys are indicative of significant crustal fractures and shears in the Särkilahti region. The largest of these is the NW-trending Pihlajavesi -fracture (Salla, 1986), which involves a magnetic and gravity anomaly low and partly limits the Särkilahti leucogranite on its NE side (Fig. 2). The migmatites in the Särkilahti region are polyphasically deformed (Salla, 1986; Nykänen, 1988). Strikes of foliation in the country rocks are often in NE-SW direction, with more or less steep dips. However, within the common NW-trending valleys the strikes of country rocks are also more typically NW-SE (see Nykänen, 1987; Lavikainen et al., 1992).

3. Sampling and analytical methods

About 70 outcrops in the Särkilahti region were mapped during 2015–2017, especially focusing on sites located at and near the leucogranite contacts. Moreover, several old field notes made in the 1980s from the study area were reviewed using the Geotietoydin database of the Geological Survey of Finland. These studies with the help of airborne geophysical data resulted in an updated view of the extent of the leucogranitic rocks (see Fig. 2), in

comparison to those given by Nykänen (1987) and Lavikainen et al. (1992). In this context, a few granodiorites of the old maps were included to the Särkilahti leucogranite. Coordinates in the Figures (except that of Fig. 1) are given in EUREF FIN TM35 FIN.

3.1. Major- and minor-element geochemistry

In addition to existing data, three new whole-rock chemical analyses were made from the Särkilahti leucogranite in the laboratory of Labtium Oy in Espoo, Finland. The leucogranite samples were crushed with a jaw crusher (Mn-steel jaws) and ground using a tungsten carbide vessel. To determine the concentration of Ba, Nb, Sr, Th, V, Y, Zr and rare earth elements (REE) (columns 1–3 in Table 1), the samples were also ground by carbide steel vessel and then were totally dissolved by an acid mix of HF-HNO_3-HCl-$HClO_4$. Analysis of the latter list of elements was carried out by inductively coupled plasma mass spectrometry (ICP-MS). All other elements (Table 1) were analysed by X-ray fluorescence (XRF) on pressed pellets. The codes used for analytical procedures in the laboratory of Labtium Oy were 175X for XRF and 308PM for ICP-MS.

3.2. U–Pb monazite geochronology

Monazite grains were located on polished 30 µm thin sections with a JEOL JSM5900LV scanning electron microscope and INCA Feature phase detection software (Oxford Instruments) at the Geological Survey of Finland, Espoo. The software performs automatic scans over a user-defined sample area and detects grains of interest based on backscattered electron intensity. Backscattered electron images of monazite grains large enough for U–Pb dating were subsequently obtained with the same instrument.

U–Pb dating of monazite was performed using a Nu Instruments AttoM single collector ICP-MS, connected to a Photon Machines Excite laser ablation (LA) system at the Finnish Geoscience Research Laboratories, Geological Survey of Finland. The analytical conditions for the laser ablation were: 15 µm beam diameter, 5 Hz pulse frequency, and 1.97 J/cm^2 beam energy density. Masses 202, 204, 206, 207, 208, 232 and 238 were measured using a single secondary electron multiplier. ^{235}U was calculated from the signal at mass 238 using a natural ^{238}U/^{235}U = 137.88. Mass number 204 was used as a monitor for common ^{204}Pb and mass 202 was monitored for Hg levels prior to and during ablation. In our ICP-MS system, ^{204}Hg almost exclusively originates from the He supply giving a background count rate on mass 204 of 200–300 cps (counts per seconds), which has been stable over the last several years. The contribution of ^{204}Hg from the plasma was eliminated by the on-mass background measurement. An in-house monazite standard A49 (TIMS age 1874±3 Ma; Salli, 1983) was used for calibration and in-house reference samples A1326 (2635±2 Ma; TIMS, Hölttä et al., 2000) and A276 (1915±3 Ma; TIMS, unpublished) were used for quality control. The age offsets from the concordant ID-TIMS results did not exceed 0.5 %. Overall, the analytical procedure was similar to that described in detail by Molnár et al. (2018).

4. Field relationships

4.1. Country rocks

An epiclastic, phlebitic garnet-cordierite-biotite migmatite is the most common country rock of the Särkilahti leucogranite. The rock has in-situ leucosome patches of various size, but it also contains irregular cross-cutting granite dykes up to some meters in width. The leucosomes and felsic dykes are in places folded. The dykes, in particular, do not contain a melanosome against the mesosome. Garnet and cordierite porphyroblasts occur in the leucosome, mesosome and granite dykes of the migmatite. These minerals are coarse grained, internally broken and locally form aggregates. The

mode of garnet and cordierite is between 1 to 20 % in total. Biotite mainly occurs in the mesosome. Its mode is up to 15 %. Sillimanite appears as an accessory mineral as well as tiny hercynite crystals.

The migmatite includes many metapsammitic, plagioclase- and quartz-dominated interlayers that contain ~ 10 % of biotite with some garnet and potassium feldspar. These less mineralogically diverse layers are medium grained and usually contain a few narrow granitic veins. Width of the layers varies from 1 cm to several meters. Their combined amount is roughly equal to the metapelitic portions in the migmatites.

In addition the bedrock contains intercalations of banded orthopyroxene-garnet paragneisses that are a few tens of meters wide (Nykänen, 1988). These pyroxene-bearing rocks are compositionally aluminium-deficient and have less leucosome compared to the rest of the migmatite. Amount of orthopyroxene in these gneisses is up to 8 %, whereas garnet mode varies from 4 to 15 % and that of biotite between 9 and 19 %. Garnet porphyroblasts are ragged and can be up to 3 cm in diameter. Potassium feldspar is usually absent in these rocks. The surface of the orthopyroxene-garnet paragneisses is slightly rusty.

Foliated even-grained, orthopyroxene-bearing metatonalites form a few areas of 0.2 to 2 km^2 in size within the migmatites and paragneisses. The metatonalites are relatively homogeneous rocks, but may contain a few granitic patches. Mode of the orthopyroxene (a metamorphic mineral in the rock) is between 1 and 5 %, biotite content ranges from 10 to 15 % but hornblende is lacking or rare (Nykänen, 1988). The fresh surface of the metatonalites is characterized by dark color, whereas weathered surface exhibits grayish colors with a rusty shade. The migmatites contain also a few small metagabbro fragments.

4.2. Leucogranite

The Särkilahti leucogranite occupies an irregular area of ~ 75 km^2 in extent (Fig. 2). Although typically more or less inhomogeneous, relatively homogeneous outcrops are encountered locally (Fig. 3). Grain size of the leucogranite is generally between 0.4 and 1 cm. In places the grain size is coarser but it may grade from coarse to medium on an individual outcrop. The leucogranite is mostly weakly deformed, although massive parts are also locally observed. Moreover, the rock contains in places vague granitic veins and patches. Gneiss xenoliths are rare except at the edge of the intrusion. The color of the rock varies from reddish gray to light gray.

The amount of potassium feldspar in the rock is high, between 40 and 50 %, rarely occurring as individual phenocrysts, 2–3 cm in size. Potassium feldspar commonly shows microscopic perthite without cross-hatched twinning. When perthite is absent, cross-hatched twinning dominates in the potassium feldspar grains. Amount of plagioclase varies from 20 to 30 %. The mineral is locally sericitized. Quartz grains (25–30 %) show shadowy extinction.

Reddish garnet grains (Ø 1–2 cm) and dark cordierite clumps (Ø 1–6 cm) are typical features of the leucogranite (Fig. 4a). The garnet is ragged; it contains rounded microscopic quartz inclusions. Garnet mode varies between 1–8 % in the rock. Cordierite-rich aggregates form elongated, centimeters long dark clumps associated with quartz and minor hercynite (Fig. 4a). Cordierite ranges in quantity from 1–8 %, but the mineral is locally pinitized. Sometimes cordierite and garnet grains have altered to a reddish brown aggregate (Fig. 4b). Biotite shows reddish pleochroism and a low modal content of between 1 and 5 %. Sillimanite usually appears as fibrolitic crystals, for example inside feldspar grains, but sometimes it also forms isolated grains 1–5 mm in length. Hercynite shows greenish pleochroism. A thin rim of sillimanite sometimes surrounds the hercynite grains. Monazite is a rather common accessory mineral in the Särkilahti leucogranite whereas zircon is less frequently observed. Some secondary muscovite and chlorite occur as accessory minerals in the granite.

Figure 3. Outcrop of moderately heterogeneous Särkilahti garnet-cordierite leucogranite (x = 602708, y = 6832803).

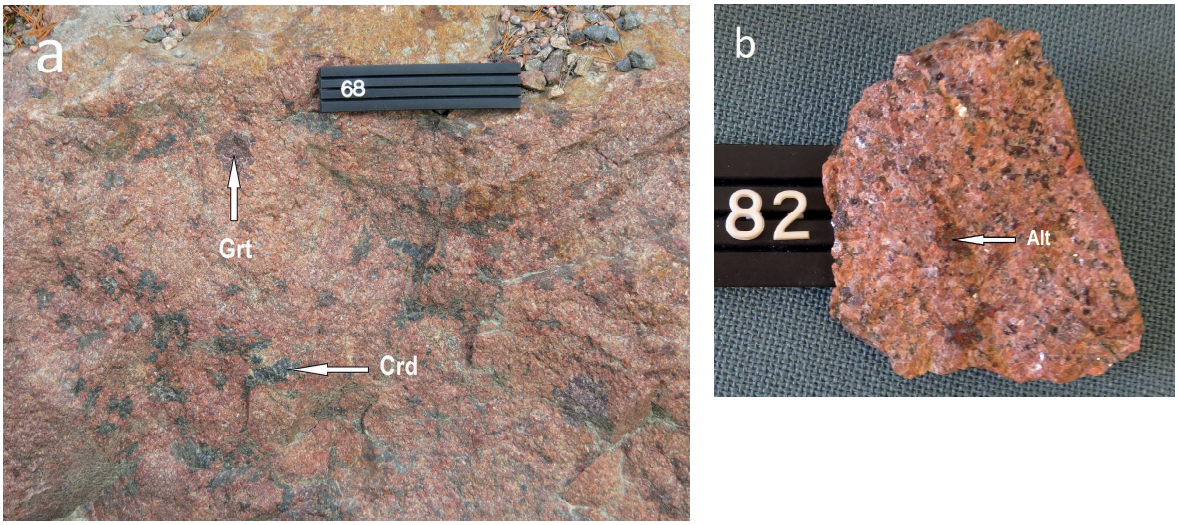

Figure 4. The Särkilahti leucogranite. a) Garnet (Grt) occurs as subrounded aggregates, whereas cordierite (Crd) with hercynite and quartz form thumb-sized aggregates (x = 602707, y = 6832803). b) Reddish brown alteration product (Alt) after cordierite in hand specimen (x = 606265, y = 6827236). Height of the sample number is 14 mm.

Figure 5. Contact between the Särkilahti leucogranite and migmatite. The leucogranite appears to have risen a short distance into the migmatite as a small antiformal structure (near the left edge) and as an axial planar intrusion in a synformal structure immediately to the right. Towards the center and right of the image small veins or sheets of leucogranite are concordant with the layering in the migmatite (x = 601534, y = 6832130). Height of the code numbers is 14 mm.

Figure 6. Contact relationships of the Särkilahti leucogranite.
a) Granitic magma penetrates the migmatitic country rock at the contact (x = 601534, y = 6832129).
b) Granite dykes inject the metatexitic country rock near the contact; cross-cutting and parallel appearances against older in-situ leucosomes (x = 602032, y = 6830104). Height of the code numbers is 14 mm.

4.3. Contact and margin of the leucogranite

The leucogranite typically has relatively sharp contacts against the country rocks. In places, the rising leucocratic magma has formed small antiformal structures (Fig. 5), but also penetrated the ductile country rock (Fig. 6a). Slightly further on the country rock side the anatectic migmatization is clearly cut by the injected leucogranitic magma (Fig. 6b). Here, the granite dykes have been injected into the country rock both parallel and perpendicularly to the trend of the migmatites. Planar fabric of the country rock has locally enabled the migration of the injecting magma. The dykes do not have clear melanosome suggesting that they are not extracted "in situ" from the local gneiss. The dykes are often pegmatitic and have slightly higher potassium feldspar/ plagioclase ratio than the in-situ leucosomes. In places these dykes and country rocks have undergone post-magmatic deformation.

Intensively melted, grey xenolith ghosts of migmatite gneiss occur at the edge of leucogranite (Fig. 7a). These sites resemble nebulitic migmatites, locally even diatexites. Margins of the leucogranite also include elongated ghost cordierite-rich relicts (Fig. 7b). In contrast, metatonalite xenolith fragments are better preserved at the margins of leucogranite. This is due to their higher melting point in relation to the migmatitic gneisses. The metatonalite fragments are usually subangular due to melting, and include abundant garnet (Fig. 7c). In addition, the marginal parts of the leucogranite may include ghost relicts of quartz-rich portions. The meters wide margin of the Särkilahti leucogranite is a heterogeneous mixture of magma and more or less melted country rock fragments.

Figure 7. Contact areas of the Särkilahti leucogranite.
a) Intensively melted garnet-cordierite-biotite migmatite xenoliths in the granite (x = 605974, y = 6927795).
b) Felsic magma surrounds ghost migmatite relicts containing dark cordierite- and hercynite-rich stripes (x = 605970, y = 6927790).
c) Subangular, garnet-bearing metatonalite xenolith in the leucogranitic garnet- and cordierite-bearing magma (x = 601534, y = 6832128). Height of the code numbers is 14 mm.

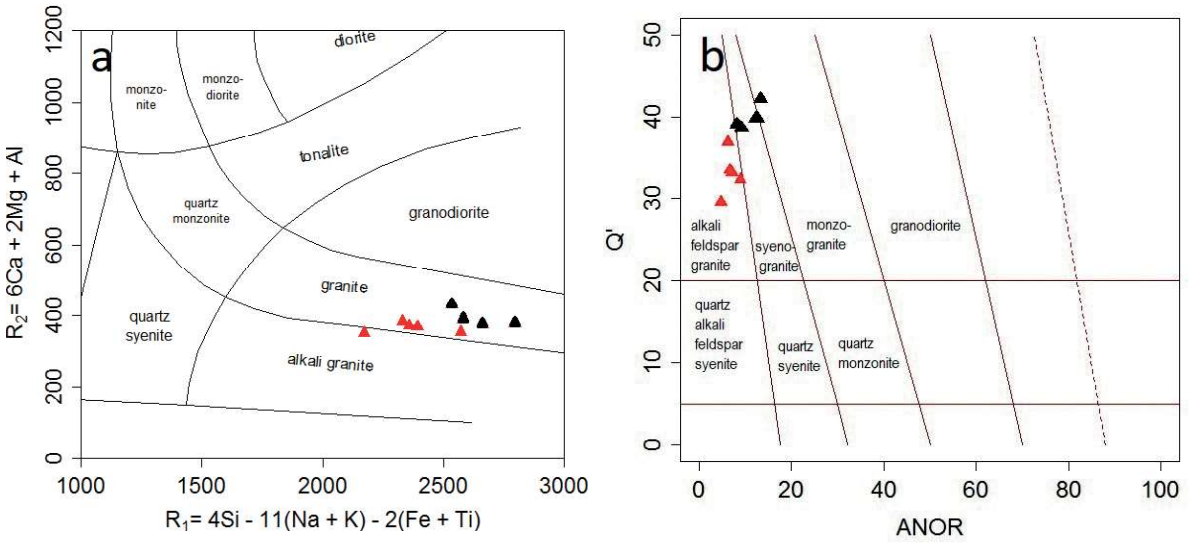

Figure 8. Discrimination diagrams for the Särkilahti leucogranite. a) R1–R2 diagram of De la Roche et al. (1980). b) Q'–ANOR diagram of Streckeisen and Lemaitre (1979) using granite mesonorms. The analyses taken from Nykänen (1988) are shown in black.

5. Chemical composition

The chemically analyzed samples from the Särkilahti leucogranite classify as granites (Fig. 8a). Using the diagram of Streckeisen and Lemaitre (1979), based on mesonorms, the samples partly plot in the alkali feldspar granite field and partly in the syenogranite field (Fig. 8b). The results agree with modal composition of the leucogranite, where potassium feldspar dominates over the two other main minerals, quartz and plagioclase.

The granites are clearly peraluminous as their aluminium saturation index (A/CNK, Shand, 1947) is between 1.09 and 1.31 (Table 1), with an average of 1.19. Using the granite discrimination diagrams of Frost et al. (2001), the leucogranite has predominantly alkali-calcic characteristics with magnesian rather than ferroan signatures.

The SiO_2 contents of the leucogranite range from 70.8 to 74.2 wt.% (Table 1). The total Fe_2O_3t + MgO + TiO_2 amount is low, less than 1.5 wt.%, except in a couple garnet- and cordierite-rich samples. Mg# of the samples is between 28 and 47. The potassium concentration is between 4.8 and 6.4 wt.%, i.e. a bit higher than typically for granites. Common fractionation index Ba/Rb ranges from 0.87 to 2.10.

In terms of Harker diagrams, only iron and titanium concentrations show relatively good correlation, in this case negative, with SiO_2. A couple chemical compositions (columns 5 and 6 in Table 1) reported by Nykänen (1988) should be treated with caution, as their analyzed total concentration of elements sum to less than 98 wt.%. Moreover, the analyses of Nykänen (1988) have slightly lower total alkali content compared to the others – which is also reflected in the discrimination diagrams (Fig. 8).

All the new samples and the earlier ones reported by Rasilainen et al. (2007) have similar and moderately elevated LREE concentrations, and display negative Eu minimum (Eu/Eu* = 0.36–0.59) (Fig. 9a). The enrichment in HREE is low and the REE pattern fractionation is strong; $(La/Yb)_N$ ranges from 31 up to 54 (Table 1). Spider diagrams for trace elements (other than REE) display peaks

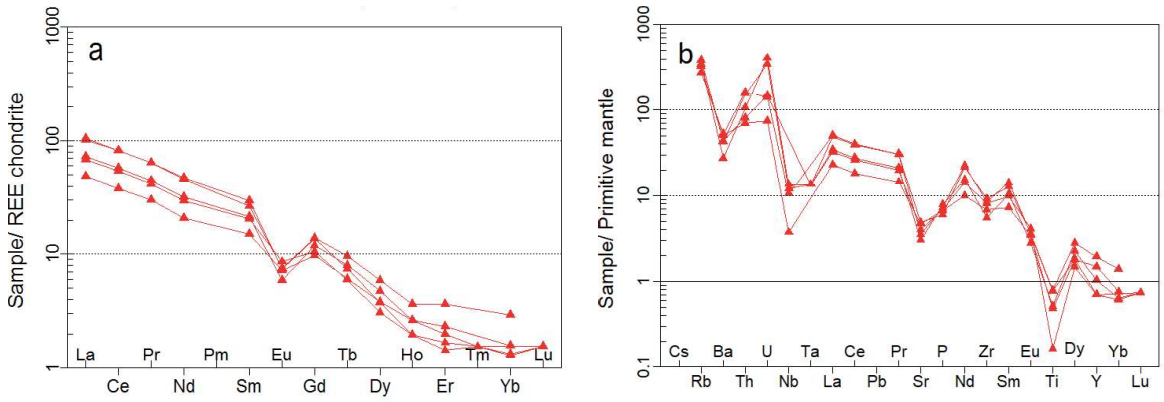

Figure 9. Spider diagrams for samples of the Särkilahti leucogranite. a) Chondrite-normalized (Boynton, 1984). b) Primitive mantle normalized after McDonough and Sun (1995).

at Rb and U, and clear troughs at Nb, Sr and Ti (Fig. 9b). There is also a negative anomaly for Ba.

Rb-content in the samples range between 165 and 232 ppm, and that of U varies 1.5 to 8.1 ppm (Table 1). In terms of quantitative contents, the concentration of Ba in the leucogranite samples varies from 180 to 346 ppm, whereas Sr contents range between 60 and 97 ppm (Table 1).

6. U–Pb age data for monazite

Abundant monazite was found in two thin sections of the Särkilahti leucogranite, 101-HMM-15 and 402-HMM-15. Monazite is mostly interstitial, or as inclusions in other minerals, most often in quartz or potassium feldspar (Fig. 10). The crystals are mostly small, euhedral, round or elongated and typically display irregular internal zoning (Fig. 11). The zoning features are usually narrower than the laser beam (15 µm), and hence most analysis spots represent mixtures of two or more zones. In Table 2, multiple analyses on the same grain are labelled a, b and c. The analysis is always closest to the center of the grain, but because of the irregular nature of the zoning, the spots do not really reflect core-rim ages.

Despite the heterogeneous appearance of the monazite crystals, both samples show relatively uniform age results (Table 2). The 21 analyses from 11 grains of sample 101-HMM-15 have a concordia age of 1780±4 Ma (Fig. 12). In sample 402-HMM-15, most analyses yielded slightly reversely discordant monazite U-Pb data. This may be due to matrix differences between the sample and standard material, unsupported uranogenic ^{206}Pb or later mobilization of U and Pb (see e.g. Corfu & Evins, 2002, or Peterman et al., 2012 for a more thorough discussion about reverse discordance in monazites). Out of the 18 analysis spots from 10 grains of 402-HMM-15, 15 are less than 5% discordant, and these yield a concordia age of 1790±6 Ma. The weighted average $^{207}Pb/^{206}Pb$ age of all 18 data points results in a comparable $^{207}Pb/^{206}Pb$ age of 1787±7 Ma (Fig. 12).

No dramatic differences were found relative to either the Th or U contents or the age in any single monazite grain. Th/U ratios range from <4 to 10, which is relatively narrow variation for monazite (e.g., Dahl et al., 2005; Borah et al., 2019). Also, whether the monazite is an inclusion or in the matrix has no significant effect on its composition or age. Hence it seems that all monazite was crystallized in a single stage, despite the heterogeneous habit.

Table 1. Chemical compositions of the Särkilahti leucogranite.

	1.	2.	3.	4.*	5.*	6.*	7.*	8.**	9.**
Sample	HMM$-2017-4.1	HMM$-2017-5.1	HMM$-2017-8.1	387b-OVN-83	415-OVN-83	326-OVN-83	314-OVN-83	92010032	92013832
SiO_2 wt%	73.21	73.76	73.07	70.75	72.44	73.10	73.70	72.9	74.2
TiO_2	0.10	0.16	0.03	0.65	0.20	0.16	0.18	0.16	0.10
Al_2O_3	14.65	14.51	14.60	14.93	14.39	13.73	14.00	14.4	14.1
Fe_2O_3t	1.02	0.89	0.55	3.01	1.48	0.86	1.07	1.10	0.84
MnO	0.01	<0.005	0.01	0.00	0.00	0.00	0.00	0.02	0.02
MgO	0.22	0.23	0.11	0.72	0.53	0.35	0.47	0.25	0.23
CaO	0.80	0.68	0.56	0.95	0.74	0.67	0.72	0.71	0.62
Na_2O	3.71	3.22	3.34	2.74	2.54	2.31	2.57	2.89	2.85
K_2O	5.13	5.78	6.39	4.76	5.56	5.46	5.57	6.16	5.71
P_2O_5	0.16	0.15	0.14	0.15	0.07	0.13	0.10	0.12	0.14
Total	99.01	99.37	98.80	98.66	97.95	96.77	98.38	98.71	98.80
A/CNK	1.12	1.13	1.09	1.31	1.25	1.26	1.21	1.13	1.18
Mg#	30	34	28	32	41	45	47	31	35
Sr ppm	60	70	80	n.a.	n.a.	n.a.	n.a.	97.0	92.6
Ba	180	280	290	n.a.	n.a.	n.a.	n.a.	346	334
Nb	8.92	7.89	<3	n.a.	n.a.	n.a.	n.a.	6.88	2.44
Y	4.4	3.0	3.0	n.a.	n.a.	n.a.	n.a.	8.29	6.41
Zr	58	88	84	n.a.	n.a.	n.a.	n.a.	95.5	71.6
U	8.12	6.95	2.95	n.a.	n.a.	n.a.	n.a.	2.79	1.48
V	5.2	6.0	<2	n.a.	n.a.	n.a.	n.a.	2.7	3.1
Th	8.41	12.3	6.47	n.a.	n.a.	n.a.	n.a.	12.9	5.57
Ta	<1	<1	<1	n.a.	n.a.	n.a.	n.a.	0.26	0.09
Sc	1.79	1.58	0.93	n.a.	n.a.	n.a.	n.a.	<2.8	<2.8
Rb	206	232	196	n.a.	n.a.	n.a.	n.a.	165	166
Co	7.32	4.47	4.47	n.a.	n.a.	n.a.	n.a.	<2.0	3.8
Zn	60	50	<20	n.a.	n.a.	n.a.	n.a.	37.7	15.0
La ppb	22.5	31.7	21.2	n.a.	n.a.	n.a.	n.a.	32.8	15.1
Ce	46.5	66.0	44.0	n.a.	n.a.	n.a.	n.a.	66.9	30.9
Pr	5.45	7.80	5.05	n.a.	n.a.	n.a.	n.a.	7.82	3.68
Nd	19.3	28.3	17.8	n.a.	n.a.	n.a.	n.a.	27.3	12.5
Sm	4.21	5.79	4.00	n.a.	n.a.	n.a.	n.a.	5.16	2.93
Eu	0.43	0.54	0.63	n.a.	n.a.	n.a.	n.a.	0.55	0.52
Gd	3.11	3.57	2.73	n.a.	n.a.	n.a.	n.a.	3.62	2.53
Tb	0.38	0.35	0.28	n.a.	n.a.	n.a.	n.a.	0.46	0.29
Dy	1.52	1.20	0.99	n.a.	n.a.	n.a.	n.a.	1.89	1.22
Ho	0.19	0.14	0.14	n.a.	n.a.	n.a.	n.a.	0.26	0.19
Er	0.42	0.30	0.35	n.a.	n.a.	n.a.	n.a.	0.77	0.49
Tm	<0.1	<0.1	<0.1	n.a.	n.a.	n.a.	n.a.	0.08	0.05
Yb	0.28	<0.2	0.28	n.a.	n.a.	n.a.	n.a.	0.62	0.33
Lu	<0.1	<0.1	<0.1	n.a.	n.a.	n.a.	n.a.	0.08	0.05
$(La/Yb)_N$	54.2	n.a.	52.9	n.a.	n.a.	n.a.	n.a.	36.0	30.7
Eu/Eu*	0.36	0.36	0.58	n.a.	n.a.	n.a.	n.a.	0.39	0.59

* From Nykänen (1988), ** from Rasilainen et al. (2007), samples 1–3 were analyzed at Labtium Oy, <0.005 = below detection limit, n.a. = not analysed, A/CNK = molecular $Al_2O_3/(CaO+Na_2O+K_2O)$, Mg# = molecular MgO/(MgO+FeOt), Eu/Eu* = EuN/SmN.

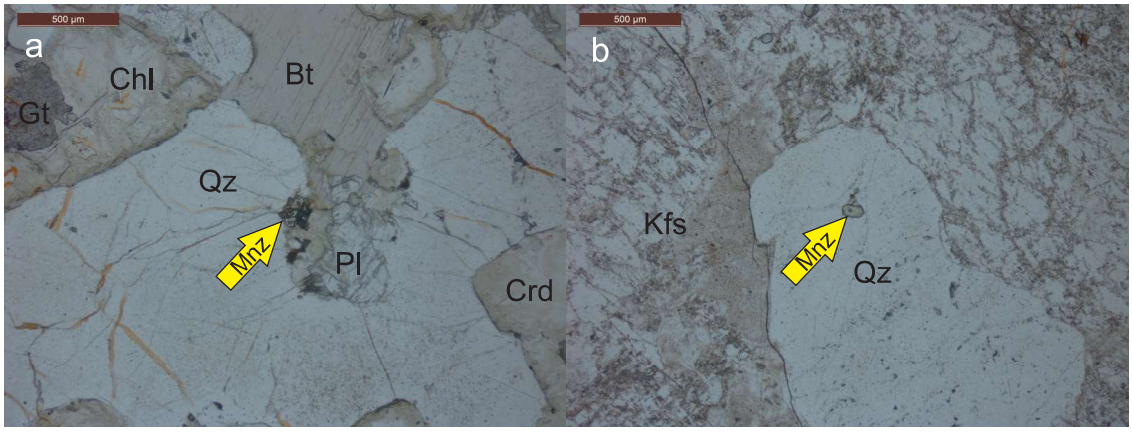

Figure 10. Microphotographs of the leucogranite. a) Interstitial monazite (Mnz) between quartz (Qz) and chloritized biotite (Bt). b) Monazite crystal (center of the image) as an inclusion in quartz. Both examples are from sample 402-HMM-15. The small round pits made by the laser beam can be seen in the monazites.

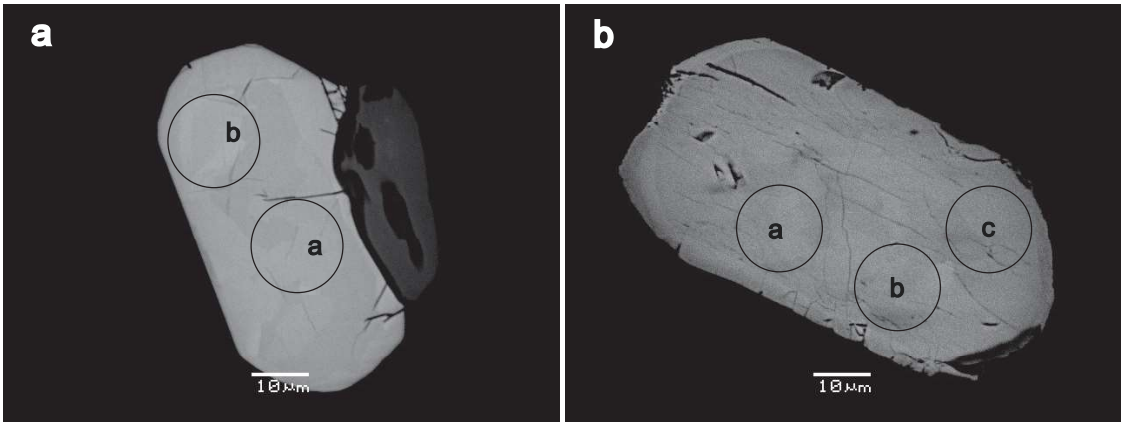

Figure 11. Backscattered electron images of the dated monazites, showing their internal heterogeneity. a) Grain 2 from sample 101-HMM-15. b) Grain 8 from sample 402-HMM-15.

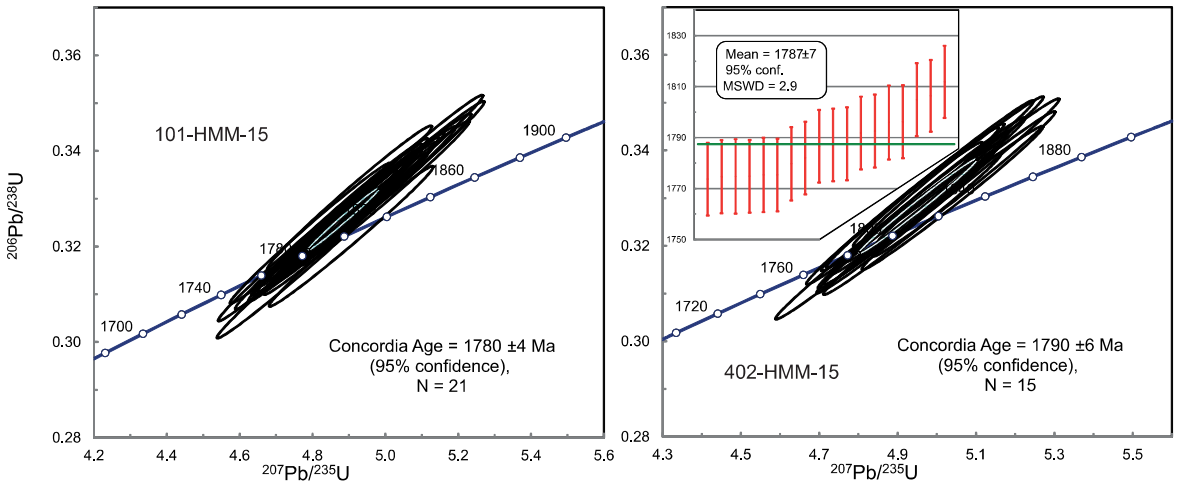

Figure 12. U–Pb concordia diagrams for the monazite of the Särkilahti leucogranite. The error ellipses and error bars are 2σ.

Table 2. Monazite U–Pb isotopic data.

		Concentration [ppm]			Radiogenic isotope ratios								Concordance	Apparent ages [Ma]					
sample	Occurrence	Pb	Th	U	$^{206}Pb/^{204}Pb$	$^{207}Pb/^{206}Pb$	1s	$^{207}Pb/^{235}U$	1s	$^{206}Pb/^{238}U$	1s	r	%	$^{207}Pb/^{206}Pb$	1s	$^{207}Pb/^{235}U$	1s	$^{206}Pb/^{238}U$	1s
101-HMM-15																			
mnz1	Incl. in qz	8531	45674	12563	96998	0.1094	0.00044	4.7561	0.1444	0.31519	0.00950	0.99	99	1790	7	1777	25	1766	46
mnz2a	Int. qz/kfs	7918	65667	6424	50020	0.1091	0.00047	4.9652	0.1509	0.33008	0.00995	0.99	103	1784	8	1813	25	1839	48
mnz2b	Int. qz/kfs	9036	61453	10222	53370	0.1091	0.00047	5.0052	0.1521	0.33265	0.01003	0.99	103	1785	8	1820	25	1851	48
mnz3a	Int. qz/plg	6402	42399	7221	64501	0.1085	0.00043	4.8089	0.1460	0.32154	0.00969	0.99	101	1774	7	1786	25	1797	47
mnz3b	Int. qz/plg	6829	44976	7895	49605	0.1082	0.00043	4.7596	0.1445	0.31893	0.00961	0.99	101	1770	7	1778	25	1784	47
mnz4a	Incl. in kfs	7034	45374	8558	51289	0.1086	0.00044	4.8615	0.1476	0.32459	0.00978	0.99	102	1776	7	1796	25	1812	47
mnz4b	Incl. in kfs	5182	39797	4643	14669	0.1086	0.00044	5.0366	0.1529	0.33635	0.01014	0.99	104	1776	7	1825	25	1869	49
mnz4c	Incl. in kfs	7344	46249	9130	77027	0.1105	0.00045	4.9065	0.1490	0.32214	0.00971	0.99	99	1807	7	1803	25	1800	47
mnz5a	Int. kfs/bt	5924	42766	5892	44406	0.1092	0.00044	4.8915	0.1485	0.32475	0.00979	0.99	101	1787	7	1801	25	1813	47
mnz5b	Int. kfs/bt	6813	44878	8041	19684	0.1088	0.00044	4.9201	0.1494	0.32786	0.00988	0.99	102	1780	7	1806	25	1828	48
mnz6a	Int. plg/chl	6760	47070	7400	90334	0.1087	0.00043	4.8462	0.1471	0.32320	0.00974	0.99	101	1779	7	1793	25	1805	47
mnz6b	Int. plg/chl	6091	43316	6495	63902	0.1077	0.00043	4.7938	0.1455	0.32277	0.00973	0.99	102	1761	7	1784	25	1803	47
mnz6c	Int. plg/chl	6136	43183	6635	50891	0.1090	0.00044	4.9135	0.1492	0.32693	0.00985	0.99	102	1783	7	1805	25	1823	48
mnz7a	Int. plg/chl	6792	42815	8186	89415	0.1095	0.00044	5.0016	0.1518	0.33122	0.00998	0.99	103	1791	7	1820	25	1844	48
mnz7b	Int. plg/chl	6424	44688	6961	61415	0.1083	0.0004	4.8774	0.1481	0.32658	0.00984	0.99	103	1771	7	1798	25	1822	48
mnz8a	Incl. in crd	8510	43651	13000	96429	0.1087	0.0004	4.8749	0.1481	0.32539	0.00981	0.99	102	1777	7	1798	25	1816	48
mnz8b	Incl. in crd	7636	46103	10241	31906	0.1091	0.0004	5.0402	0.1531	0.33511	0.01010	0.99	104	1784	7	1826	25	1863	49
mnz9	Incl. in qz	6432	47217	6825	69181	0.1085	0.0004	4.8548	0.1475	0.32460	0.00978	0.99	102	1774	7	1794	25	1812	47
mnz10	Int. qz/kfs	7213	49696	8364	136199	0.1077	0.0005	4.9019	0.1491	0.33022	0.00995	0.99	104	1760	8	1803	25	1839	48
mnz11a	Incl. in plg	6068	44278	6300	81560	0.1083	0.0004	4.8912	0.1486	0.32770	0.00988	0.99	103	1770	7	1801	25	1827	48
mnz11b	Incl. in plg	6397	46960	6583	125198	0.1088	0.0004	4.9343	0.1499	0.32886	0.00991	0.99	103	1780	7	1808	25	1833	48
402-HMM-15																			
mnz1a	Int. kfs/plg	8334	44656	9821	33672	0.1108	0.00043	5.0401	0.1530	0.33004	0.00995	0.99	101	1812	7	1826	25	1839	48
mnz1b	Int. kfs/plg	7461	48445	6752	15923	0.1086	0.00043	4.8917	0.1485	0.32682	0.00985	0.99	102	1775	7	1801	25	1823	48
mnz2a	Int. qz/glue	9388	53695	10197	98734	0.1085	0.00043	5.0932	0.1546	0.34039	0.01026	0.99	106	1775	7	1835	25	1889	49
mnz2b	Int. qz/glue	7914	47838	8344	124589	0.1098	0.00044	5.0795	0.1542	0.33555	0.01011	0.99	104	1796	7	1833	25	1865	49
mnz3	Int. qz/chl	9430	43083	12930	99031	0.1104	0.00043	5.0696	0.1538	0.33298	0.01003	0.99	102	1806	7	1831	25	1853	48
mnz4	Incl. in crd	7095	45991	6532	73869	0.1085	0.00042	5.1063	0.1550	0.34125	0.01028	0.99	106	1775	7	1837	25	1893	49
mnz5a	Int. chl/gt	8856	51775	9592	115272	0.1090	0.00043	5.1441	0.1561	0.34243	0.01032	0.99	106	1782	7	1843	25	1898	49
mnz5b	Int. chl/gt	8169	52582	7638	84489	0.1088	0.00043	5.0409	0.1530	0.33597	0.01012	0.99	105	1780	7	1826	25	1867	49
mnz6	Incl. in bt	7330	43081	8007	44591	0.1098	0.00043	4.9192	0.1493	0.32492	0.00979	0.99	101	1796	7	1806	25	1814	47
mnz7a	Int. plg/kfs	7762	48428	8445	84280	0.1092	0.00043	4.9969	0.1516	0.33179	0.01000	0.99	103	1787	7	1819	25	1847	48
mnz7b	Int. plg/kfs	7282	49688	6775	53823	0.1086	0.00042	5.0173	0.1523	0.33520	0.01010	0.99	105	1775	7	1822	25	1864	49
mnz8a	Incl. in kfs	6486	45752	5988	88357	0.1093	0.00043	4.8093	0.1460	0.31916	0.00962	0.99	100	1788	7	1787	25	1786	47
mnz8b	Incl. in kfs	7108	45070	7708	90201	0.1095	0.00043	4.9227	0.1494	0.32593	0.00982	0.99	101	1792	7	1806	25	1819	48
mnz8c	Incl. in kfs	6858	44408	7276	103329	0.1093	0.00043	4.9565	0.1504	0.32902	0.00991	0.99	102	1787	7	1812	25	1834	48
mnz9a	Int. qz/bt/chl	6833	44406	7446	124060	0.1103	0.00043	4.9373	0.1498	0.32456	0.00978	0.99	100	1805	7	1809	25	1812	47
mnz9b	Int. qz/bt/chl	6844	49702	6188	57970	0.1085	0.00043	4.9453	0.1501	0.33052	0.00996	0.99	104	1775	7	1810	25	1841	48
mnz9c	Int. qz/bt/chl	6556	39298	7543	136073	0.1085	0.00042	4.9313	0.1497	0.32975	0.00994	0.99	103	1774	7	1808	25	1837	48
mnz10	Incl. in qz	6734	45499	6625	49887	0.1096	0.00043	4.9388	0.1499	0.32686	0.00985	0.99	101	1793	7	1809	25	1823	48

Abbreviations: Int. - interstitial, Incl. - inclusion, bt - biotite, chl - chlorite, crd - cordierite, gt - garnet, kfs - alkali feldspar, plg - plagioclase, qz - quartz, r - rho=correlation of $^{207}Pb/^{235}U$ and $^{206}Pb/^{238}U$ errors

7. Discussion

7.1. Emplacement of the leucogranite

As already stated, the Särkilahti leucogranite is a part of a widespread melt-forming event in the crust – demonstrably by the very many related granite intrusions and bodies in the 100 km wide and 500 km long granite-migmatite zone of southern Finland. This mostly upper amphibolite to granulite facies anatectic terrain indicates that huge heat flux has passed into the crust. The edge areas of the Särkilahti leucogranite contain intensively melted xenoliths, but the migmatitic country rocks nearby also include cross-cutting granite dykes.

We suggest that the Särkilahti leucogranite represents the exhumed upper part of an extensive "magma layer", the upper surface of which can be named as MI (magma interface) in the crust (Fig. 13) – with reference to the concept presented by Chen and Grapes (2007; figs. 3.12 & 3.13). That is to say, the leucogranite should not be seen as an upwards accumulated (via feed channels) magma in the crust. In the formation model proposed (Fig. 13), restites have sunk down to form their own layer at the bottom of the magma layer (see also Chen & Grapes, 2007; fig. 3.12). The leucogranite layer develops when the dense residual fraction in the most melted part of the anatectic region sinks and displaces the less dense leucogranite fraction upwards; this may be viewed as a form of single episode convection (see also Chen & Grapes, 2007, fig. 3.12). In effect the extensively melted layer becomes stratified with melt at the top. This process occurred after peak melting and likely continued during crystallization enabling the leucogranitic melt to develop its somewhat fractionated K_2O-rich bulk composition.

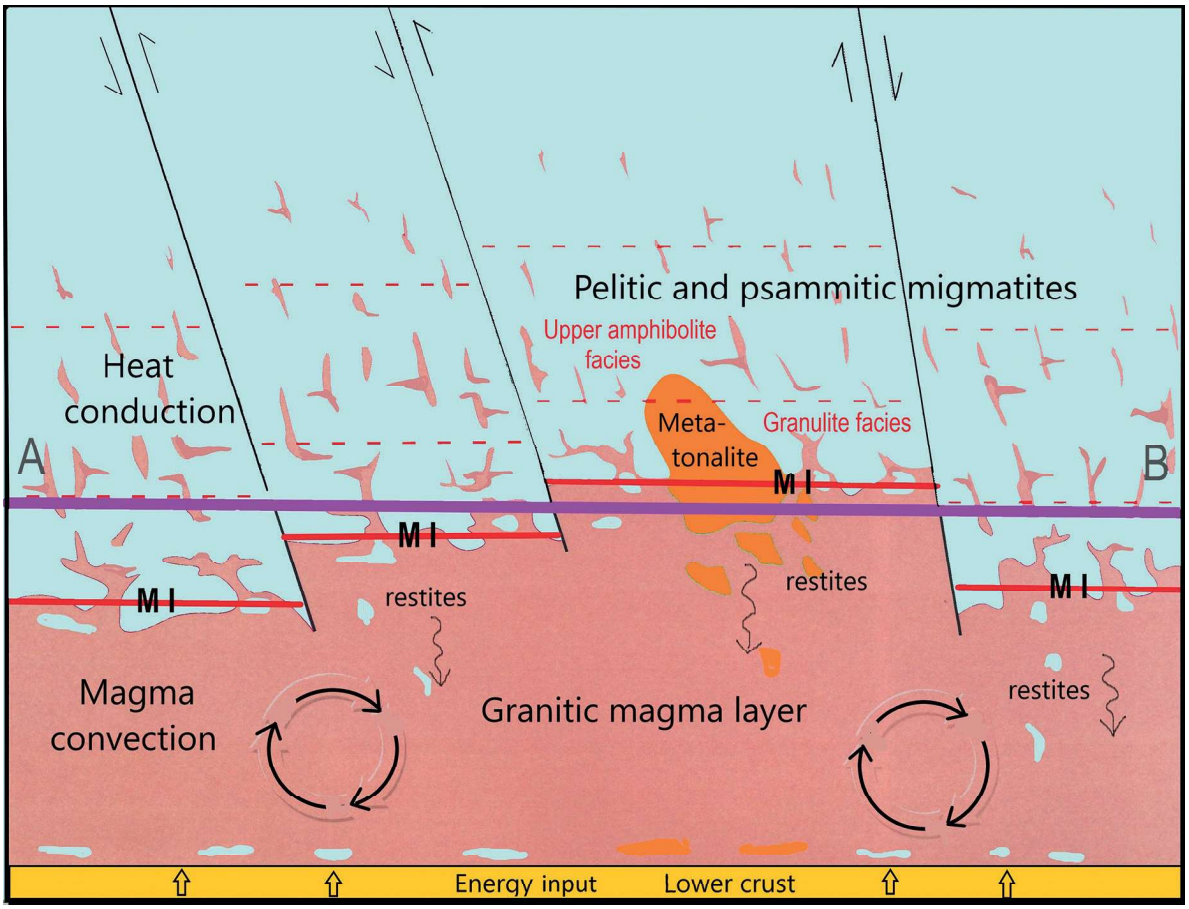

Figure 13. Schematic crustal section of the Särkilahti region following line A-B in Figure 2. The present erosional surface is marked by lilac line. The MI (magma interface) separates the convecting magma layer from the zone above, where partial melting (formation of in-situ leucosomes) occurs due to upward conduction of heat. Red dotted lines illustrate present metamorphic isograds. No vertical scale, but the MI represents depth of 15–20 km, and the bottom of magma layer refers to 20–25 km.

Due to the constant input of thermal energy, the magma interface (MI) slowly moves upwards accompanied by increasing thickness of the magma layer – by melting the roof rock (Figs. 5 & 7a-c) (see Chen & Grapes, 2007). Granite magma can enhance some melting of hot country rock if it also brings H_2O (Schwindinger & Weinberg, 2017). In addition, short-range penetration of magma may occur at the MI (Fig. 6a). The cross-cutting granite dykes in the slightly earlier formed, above migmatites (Fig. 6b) represent late-stage crystallization products of the magma layer (Fig. 13).

The following observations support the formation model of the magma layer: there is no contact metamorphic aureole nor feed channels found around the Särkilahti leucogranite, but regional scale, practically contemporaneous granulite-grade terrain (referred to below). Moreover, chemical composition of the leucogranite, such as only moderately elevated Rb/Ba, indicate that the magma is not highly fractionated.

Geological observations reported from the well-studied granulite-grade Sulkava region nearby (e.g. Korsman et al., 1984), which also belongs to the extensive granite-migmatite zone of southern Finland, support the proposed emplacement model for the Särkilahti leucogranite. The following citations clarify the issue. First, "…migmatising potas-

sium granite shows intrusive features…" (Korsman, 1977). Secondly, "…the formation of the Sulkava thermal dome ……cannot be attributed to a tectonically thickened crust alone…", and "…the isograd surfaces are ……likely to be almost horizontal…", and "…metamorphism culminated between 1850 and 1810 Ga ago…" (Korsman et al., 1984).

7.2. Metamorphism of the country rocks

According to Kurhila et al. (2011), zircon in leucosomes of the garnet-cordierite migmatite at Säviönsaari (30 km NW from Särkilahti) crystallized c. 1.83 Ga ago and monazite grains c. 1.80 Ga. In the Karhukoski area, 20 km west of Särkilahti, monazite in a related migmatite crystallized c. 1.80 Ga ago (Nykänen, 1988). According to Korsman and Kilpeläinen (1986), garnet and cordierite did not attain equilibrium in the migmatites of the Sulkava region until after the D3 deformation, i.e. relatively late in the tectonomagmatic evolution. These data show that the peak of regional metamorphism in country rocks and the crystallization of the Särkilahti leucogranite (1.79–1.78 Ga, see Chapter 6) are almost contemporaneous, the leucogranite being slightly younger. Thus, the in-situ leucosomes and the cross-cutting granite dykes shown in Figure 6b do not represent two distinct metamorphic events, but one longer lasting event. The afore-mentioned data also suggest that the granite layer did not crystallize in cool country rocks.

The metatexitic country rocks located above the magma layer have been metamorphosed by heat flow conduction (see Fig. 13). The in-situ leucosomes of these migmatites do not have "roots" into the magma layer. These leucosomes formed during metamorphic peak. Further above, the metamorphic grade should be lower, as the amount of conducted heat was smaller. In other words, the metamorphic isograds should have been more or less horizontal above the suggested magma layer. Crystallization of metamorphic orthopyroxene in the compositionally aluminium-deficient paragneisses and in the metatonalites indicate that the adjacent country rocks of the Särkilahti leucogranite have been metamorphosed in granulite facies. The huge regional energy input (heat flux) from mantle is the original cause for the metamorphism and melting in the crust.

Anatectic melts formed in a granulite-grade metamorphic deep environment do not necessarily rise through the continental crust to form plutons (e.g. Cruden, 2006). In fact, granulite-grade metamorphism and the injection of veins in country rocks can be contemporaneous, that is to say granulite facies terrains can be enriched in melt, i.e. not melt-depleted (Morfin et al., 2013). Numerous leucosomes in the Särkilahti garnet-cordierite-biotite migmatites indicate an enrichment of a melt phase rather than melt-depleted environment.

During the crustal uplift and final domain exhumation, the uppermost rocks (i.e. the less metamorphosed, see Fig. 13) cooled first, followed later by the granulite-grade migmatites (c. 1.80 Ga). Finally, the below lain Särkilahti leucogranite cooled 1.79–1.78 Ga ago. The migmatites had much less melt and effectively stop growning datable minerals earlier than the leucogranite, which did not stop growning datable minerals until solidus.

Because fracture zones partly limit the Särkilahti leucogranite, the present surface may also partly be due to postorogenic subvertical block movements (cf. Figs. 2 & 13). This is suggested because southwest of the study area, and behind the NW-trending shear zones, the metamorphic grade is a bit lower as indicate by the absence of metamorphic orthopyroxene in the paragneisses and metatonalites (see Nykänen, 1987, 1988).

7.3. Source of the granitic magma

The Särkilahti leucogranite is derived from its country rocks. Field observations show that the country rock is composed of metapelitic and -psammitic interlayers in ~ 50 – 50 % amounts. According to this ratio, we can roughly calculate

the chemical composition of the metasedimentary country rock by combining the mean of two average chemical compositions: (1) the garnet-cordierite-biotite migmatite ("kinzigites") and (2) the metapsammitic layers ("quartz feldspar gneisses/greywackes") whose chemical compositions are given by Nykänen (1988) and Rasilainen et al. (2007). This calculation produces the following average chemical composition for the migmatitic country rock: 66.6 wt.% SiO_2, 0.6 wt.% TiO_2, 16.8 wt.% Al_2O_3, 5.3 wt.% FeOt, 0.1 wt.% MnO, 1.7 wt.% MgO, 1.9 wt.% CaO, 2.4 wt.% Na_2O and 2.9 wt.% K_2O. If we further speculate that some of the titanium, iron, magnesium and calcium of the migmatites and interlayers will be sequestered and removed from the magma during melting of restites (see Fig. 13), the remaining composition starts to resemble that of the Särkilahti leucogranite, except too small K-content (cf. Table 1). With reference to the latter, the elevated potassium concentration in the leucogranite can be explained by convection in the magma layer (Fig. 13).

According to experimental data on rock melting, rather small chemical differences in metasedimentary source material can have a large influence on the composition of the melt formed (e.g. Chen & Grapes, 2007, and references there in). For certain, pelitic-psammitic sedimentary rocks cannot produce over 50 % of granite melt in normal granulite-grade conditions (e.g. Vielzeuf & Holloway, 1988; Chen & Grapes, 2007), the remaining part being restites with some granodioritic and tonalitic melts. The Särkilahti leucogranite does not contain tonalite phases, nor is it isochemically similar to the country rocks. As mentioned, the magma layer concept of Chen and Grapes (2007) includes thermal convection; separation of non-fusible, dense tonalite blocks and related Fe- and Mg-rich restites from the roof of the layer, and their gravitational differentiation as xenoliths move downwards within the magma could contribute to the light leucocratic granitic melt rising upwards (Fig. 13).

7.4. Alternative emplacement models

Stålfors and Ehlers (2006) have illustrated that some granites in the western part of the granite-migmatite zone of southern Finland were transported upwards along subvertical shear zones and were emplaced as subhorizontal sheets. The Särkilahti leucogranite represents a much larger body than the afore-mentioned sheets (width ≤ 25 m), and its SW contact is usually not sheared (see Figs. 5 & 6). It should also be noted that the country rocks of the Särkilahti leucogranite are metamorphosed in granulite facies, not in upper amphibolite facies conditions, which characterize many other areas in the granite-migmatite zone of southern Finland. In other words, the present erosional surface at the Särkilahti region evidently represents slightly deeper crustal section in comparison to many other locations in the granite-migmatite zone of southern Finland.

Although the Särkilahti leucogranite is only one granite area in the 100 km wide and 500 km long granite-migmatite zone of southern Finland, the granites of the zone should have something common in terms of crustal scale formation mechanism and emplacement. This is supported by the fact that these granites are usually hosted by rocks that have partially melted in the upper amphibolite or granulite facies. Naturally, there are local variations due to such things as local structural details, variations in mantle heat flow into the base of the crust, different rock types present and its effect on melt production/fertility, thermal conductivity and radiogenic heat production.

8. Conclusions

In summary from above, we draw the following conclusions from this study:

– The Särkilahti leucogranite does not represent an accumulated magma that ascended (via network of channels) upwards to a cooler crustal environment, nor do the anatectic in-situ

leucosomes and cross-cutting granite dykes in migmatitic country rocks refer to melts below a large granite body.
– The proposed extensive horizontal magma layer – now partly exhumed as the leucogranite – has slowly risen upwards and at its upper limit (MI, magma interface) melted the granulite-grade roof rocks by associated heat flux (Fig. 13). Higher in the system, the rising heat conduction transformed country rocks to upper-amphibolite facies migmatites rich in in-situ leucosomes. Late-stage crystallization products of the layer gave rise to pegmatitic granite dyke injections in the slightly earlier formed migmatites above. Thus the leucosomes and injecting dykes in the migmatites are the result of one long-time thermal event.
– Within the magma layer, lighter granitic melt ascended as a consequence of the residue sinking. These convections caused the formation of a more felsic upper stratified layer, the Särkilahti leucogranite.
– During final uplift and cooling of the crust, the above migmatites crystallized first (1.83–1.80 Ga), followed a bit later (1.79–1.78 Ga ago) by the deeper magma layer, the Särkilahti leucogranite.
– The emplacement model presented in this article could be applied to related, irregular granite areas in the 100 km wide and 500 km long granite-migmatite zone of southern Finland.

Acknowledgements

We thank Raimo Lahtinen for inspiring comments on the manuscript. Sari Lukkari is warmly thanked for the automated searching and subsequent documenting (Fig. 11) of the monazite grains for U–Pb analyses. Harri Kutvonen and Anneli Lindh kindly assisted in the formulation of the figures, a work which is appreciated. We also thank Ed Sawyer and one anonymous reviewer for their good comments, which significantly improved the manuscript.

References

Borah, P., Hazarika, P. Mazumdar, A.C. & Rabha, M., 2019. Monazite and xenotime U–Th–Pb total ages from basement rocks of the (central) Shillong–Meghalaya Gneissic Complex, Northeast India. Journal of Earth System Science 128: 68. https://doi.org/10.1007/s12040-019-1085-x

Boynton, W.V., 1984. Cosmochemistry of the rare earth elements: Meteorite studies. In: Henderson, P.J. (ed.) Rare Earth Element Geochemistry; Developments in Geochemistry 2. Amsterdam: Elsevier. pp. 505–535. https://doi.org/10.1016/B978-0-444-42148-7.50008-3

Brown, M., 2013. Granite: From genesis to emplacement. Bulletin of the Geological Society of America 125, 1079–113. https://doi.org/10.1130/B30877.1

Chen, G.-N. & Grapes, R., 2007. Granite genesis: In-Situ Melting and Crustal Evolution. Springer-Verlag, Dordrecht. 278 p. https://doi.org/10.1017/S0016756809006189

Corfu, F. & Evins, P.M., 2002. Late Palaeoproterozoic monazite and titanite U–Pb ages in the Archaean Suomujärvi Complex, N-Finland. Precambrian Research 116, 171–181. https://doi.org/10.1016/S0301-9268(02)00024-4

Cruden, A.R., 2006. Emplacement and growth of plutons: implications for rates of melting and mass transfer in continental crust. In: Brown, M., Rushmer, T. (eds), Evolution and Differentiation of the Continental Crust. Cambridge University Press. pp. 455–519.

Dahl, P.S., Hamilton, M.A., Jercinovic, M.J., Terry, M.P., Williams, M.L. & Frei, R., 2005. Comparative isotopic and chemical geochronometry of monazite, with implications for U-Th-Pb dating by electron microprobe: An example from metamorphic rocks of the eastern Wyoming Craton (U.S.A.). American Mineralogist 90, 619–638. https://doi.org/10.2138/am.2005.1382

De la Roche, H., Leterrier, J., Granclaude, P. & Marchal, M., 1980. A classification of volcanic and plutonic rocks using R1–R2 diagrams and major element analyses – its relationships and current nomenclature. Chemical Geology 29, 183–210. https://doi.org/10.1016/0009-2541(80)90020-0

Ehlers, C., Lindroos, A. & Selonen, O., 1993. The late Svecofennian granite-migmatite zone of southern Finland – a belt of transpressive deformation and granite emplacement. Precambrian Research 64, 295–309. https://doi.org/10.1016/0301-9268(93)90083-E

Frost, B.R., Barnes, C.G., Collins, W.J., Arculus, R.J., Ellis, D.J. & Frost C.D., 2001. A Geochemical Classification for Granitic Rocks. Journal of Petrology 42, 2033–2048. https://doi.org/10.1093/petrology/42.11.2033

Hobbs, B.E. & Ord, A., 2010. The mechanics of granitoid systems and maximum entropy production rates. Philosophical Transactions of the Royal Society. A. Mathematical, Physical and Engineering Sciences 368, 53–93. https://doi.org/10.1098/rsta.2009.0202

Hölttä, P., Huhma, H., Mänttäri, I. & Paavola, J., 2000. P-T-t development of Archaean granulites in Varpaisjärvi, Central Finland, II: Dating of high-grade metamorphism with the U–Pb and Sm–Nd methods. Lithos 50, 121–136. https://doi.org/10.1016/S0024-4937(99)00055-9

Hölttä, P. & Heilimo, E., 2017. Metamorphic map of Finland. In: Nironen, M. (ed.), Bedrock of Finland at the scale 1:1 000 000 – Major stratigraphic units, metamorphism and tectonic evolution.

Johannes, W., Ehlers, C., Kriegsman, L.M. & Mengel, K., 2003. The link between migmatites and S-style granites in the Turku area, southern Finland. Lithos 68, 69–90. https://doi.org/10.1016/S0024-4937(03)00032-X

Korsman, K., 1977. Progressive metamorphism of the metapelites in the Rantasalmi-Sulkava area, southeastern Finland. Geological Survey of Finland, Bulletin 290, 82 p.

Korsman, K. & Kilpeläinen, T., 1986. Relationship between zonal metamorphism and deformation in the Rantasalmi-Sulkava area, southeastern Finland. In: Korsman, K. (ed.), Development of deformation, metamorphism and metamorphic blocks in eastern and southern Finland. Geological Survey of Finland, Bulletin 339, pp. 33–42.

Korsman, K., Hölttä, P., Hautala, T. & Wasenius, P., 1984. Metamorphism as an indicator of evolution and structure of the crust in Eastern Finland. Geological Survey of Finland, Bulletin 328, 40 p.

Korsman, K. (ed.), Koistinen, T. (ed.), Kohonen, J. (ed.), Wennerström, M. (ed.), Ekdahl, E. (ed.), Honkamo, M. (ed.), Idman, H. (ed.) & Pekkala, Y. (ed.), 1997. Suomen kallioperäkartta = Berggrundskarta över Finland = Bedrock map of Finland 1:1 000 000. Geological Survey of Finland.

Korsman, K., Korja, T., Pajunen, M., Virransalo, P. & GGT/SVEKA Working Group, 1999. The GGT/SVEKA Transect: Structure and evolution of the continental crust in the Paleoproterozoic Svecofennian orogen in Finland. International Geology Review 41, 287–333. https://doi.org/10.1080/00206819909465144

Kukkonen, I.T. & Lauri, L.S., 2009. Modelling the thermal evolution of a collisional Precambrian orogen: High heat production migmatitic granites of southern Finland. Precambrian Research 168, 233–246. https://doi.org/10.1016/j.precamres.2008.10.004

Kurhila, M., Vaasjoki, M., Mänttäri, I., Rämö; T. & Nironen, M., 2005. U–Pb ages and Nd isotope characteristics of the lateorogenic, migmatizing microcline granites in southwestern Finland. Bulletin of the Geological Society of Finland 77, 105–128. https://doi.org/10.17741/bgsf/77.2.002

Kurhila, M., Mänttäri, I., Vaasjoki, M., Rämö; O.T. & Nironen, M., 2011. U–Pb geochronological constrains of the late Svecofennian leucogranites of southern Finland. Precambrian Research 190, 1–24. https://doi.org/10.1016/j.precamres.2011.07.008

Lahtinen, R., Korja, A. & Nironen, M., 2005. Paleoproterozoic tectonic evolution. In: Lehtinen, M., Nurmi, P.A. & Rämö, T. (eds.), Precambrian Geology of Finland – Key to the Evolution of the Fennoscandian Shield. Elsevier B.V., Amsterdam, pp. 481–532. https://doi.org/10.1016/S0166-2635(05)80012-X

Lavikainen, S., Pakkanen, L. & Salla, A., 1992. Lohilahti. Geological map of Finland 1:100 000, pre-Quaternary rocks, sheet 4122. Geological Survey of Finland.

Luukas, J., Kousa, J., Nironen, M. & Vuollo, J., 2017. Major stratigraphic units in the bedrock of Finland, and an approach to tectonostratigraphic division. In: Nironen, M. (ed.) 2017, Bedrock of Finland at the scale 1:1 000 000 – Major stratigraphic units, metamorphism and tectonic evolution. Geological Survey of Finland, Special Paper 60, pp. 9–40.

Mäkitie, H., O'Brien, H., Selonen, O. & Lukkari, S., 2016. Formation mechanism and age of the Särkilahti garnet-cordierite leucogranite, SE Finland. 32. Nordic Geological Winter Meeting, 13th–15th January 2016, Helsinki, Finland, Bulletin of the Geological Society Finland, Special Volume, p. 228.

McDonough, W.F. & Sun, S.S., 1995. The composition of the Earth. Chemical Geology 120, 223–253. https://doi.org/10.1016/0009-2541(94)00140-4

Molnár, F., Middleton, A., Stein, H., O'Brien, H., Lahaye, Y., Huhma, H., Pakkanen, L. & Johanson, B., 2018. Repeated syn- and post-orogenic gold mineralization events between 1.92 and 1.76 Ga along the Kiistala Shear Zone in the Central Lapland Greenstone Belt, northern Finland. Ore Geology Reviews 101, 936–959. https://doi.org/10.1016/j.oregeorev.2018.08.015

Morfin, S., Sawyer, E.W. & Bandyayera, D., 2013. Large volumes of anatectic melt retained in granulite facies migmatites: An injection complex in northern Quebec. Lithos 168-169, 200–218. https://doi.org/10.1016/j.lithos.2013.02.007

Nironen, M., 2017. Guide to the Geological Map of Finland – Bedrock 1:1 000 000. In: Nironen (ed.), Bedrock of Finland at the scale 1:1 000 000 – Major stratigraphic units, metamorphism and tectonic evolution. Geological Survey Finland, Special Paper 60, pp. 41–76.

Nironen, M. & Kurhila, M., 2008. The Veikkola granite area in southern Finland: emplacement of a 1.83–1.82 Ga plutonic sequence in an extensional regime. Bulletin of the Geological Society of Finland 80, 39–68. https://doi.org/10.17741/bgsf/80.1.003

Nironen, M., Kousa, J., Luukas, J. & Lahtinen, R. (eds.), 2016. Suomen geologinen kartta: kallioperä – Geologisk karta över Finland: berggrund – Geological Map of Finland: Bedrock 1:1 000 000. Geological Survey of Finland.

Nurmi, P. & Haapala, I., 1986. The Proterozoic granitoids of Finland: granite types, metallogeny and relation to crustal evolution. Bulletin of the Geological Society of Finland 58, 203–233.

Nykänen, O., 1987. Virmutjoki. Geological map of Finland 1:100 000, pre-Quaternary rocks, sheet 4121. Geological Survey of Finland.

Nykänen, O., 1988. Virmutjoki. Explanation to the Geological map of Finland 1:100 000, pre-Quaternary rocks, sheet 4121. Geological Survey of Finland. 64 p (in Finnish with English summary).

Peterman, E.M., Mattinson, J.M. & Hacker, B.R., 2012. Multi-step TIMS and CA-TIMS to monazite U–Pb geochronology. Chemical Geology 312–313, 58–73. https://doi.org/10.1016/j.chemgeo.2012.04.006

Rasilainen, K., Lahtinen, R. & Bornhorst, Th., 2007. The Rock Geochemical Database of Finland. Geological Survey of Finland, Report of Investigation 164, 38 p.

Salla, A., 1986. [Findings from the bedrock of the Lohilahti (4122) map area]. Havaintoja Lohilahden (4122) kartta-alueen kallioperästä. Geological Survey of Finland, report K/41217-86/1. 16 p. (in Finnish)

Salli, I., 1983. Pielavesi. Explanation to the Geological map of Finland 1:100 000, pre-Quaternary rocks, sheet 3314. Geological Survey of Finland. 29 p. (in Finnish with English summary)

Schwindinger, M. & Weinberg, R.F., 2017. A felsic MASH zone of crustal magmas – Feedback between granite magma intrusion and *in situ* crustal anatexis. Lithos 284-285, 109–121. https://doi.org/10.1016/j.lithos.2017.03.030

Selonen, O., 1988. [Geology of the Särkilahti area, SE Finland]. Geologin inom Särkilahti-området, SE Finland. M.Sc. Thesis, Åbo Akademi University, Finland, 104 p. (in Swedish)

Selonen, O. & Ehlers, C. & Lindroos, A., 1996. Structural features and emplacement of the late Svecofennian Perniö granite sheet in southern Finland. Bulletin of the Geological Society of Finland 68, 5–17. https://doi.org/10.17741/bgsf/68.2.001

Shand, S.J., 1947. Eruptive rocks. Their Genesis, Composition, Classification and their relation to Ore Deposits. 3rd. edition. Wiley & Sons, New York, 448 p.

Stålfors, T. & Ehlers, C., 2006. Emplacement mechanisms of late-orogenic granites: structural and geochemical evidence from southern Finland. International Journal of Earth Sciences 95, 557–568. https://doi.org/10.1007/s00531-005-0049-3

Streckeisen, A. & Lemaitre, R.W., 1979. A chemical approximation to the modal QAPF classification of the igneous rocks. Neues Jahrbuch für Mineralogie, Abhandlungen 136, 169–206.

Väisänen, M., Mänttäri, P. & Hölttä, P., 2002. Svecofennian magmatic and metamorphic evolution in southwestern Finland as revealed by U-Pb zircon SIMS geochronology. Precambrian Research 116, 111–127. https://doi.org/10.1016/S0301-9268(02)00019-0

Vielzeuf, D. & Holloway, J.R., 1988. Experimental determination of the fluid-absent melting relations in the pelitic system. Consequences for crustal differentiation. Contributions to Mineralogy and Petrology 98, 257–76. https://doi.org/10.1007/BF00375178